*Sensors & Transducers, Vol. 210, Issue 3, March 2017, pp. 1-8*

www.sensorsportal.com

**Sensors & Transducers**

Published by IFSA Publishing, S. L., 2017
http://www.sensorsportal.com

# Flexural, Viscoelastic and Thermal Properties of Epoxy Polymer Composites Modified with Cellulose Nanofibers Extracted from Wheat Straw

**Md. Nuruddin, * Mahesh HOSUR, Tanjheel MAHDI, Shaik JEELANI**
Department of Materials Science and Engineering,
Tuskegee University, Tuskegee, AL-36088, USA
Tel.: +1334-724-4220, fax: +1334-724-4220
* E-mail: hosur@mytu.tuskegee.edu

*Received: 9 January 2017 /Accepted: 28 February 2017 /Published: 31 March 2017*

**Abstract:** The objective of this study is to extract cellulose nanofibers (CNFs) from wheat straw and utilize them in thermoset polymers to improve their performance. CNFs were extracted from wheat straw by formic/peroxyformic acid treatment, hydrogen peroxide bleaching, followed by ball milling. To ensure better interaction between CNFs and epoxy polymer matrix, surface of CNFs was chemically modified by silane treatment. Furthermore, surface treated CNFs were added in varying proportion (1, 2 and 3 %) to an epoxy polymer to fabricate polymer composites. The chemical reaction and structural analysis was evaluated by FTIR analysis. Incorporation of CNFs into matrix increased flexure strength, flexure modulus, storage modulus, glass transition temperature and decomposition temperatures. Maximum improvement was observed for 2 % loading of CNFs as it facilitates maximum crosslinking with epoxy polymers. Maximum improvement in flexure strength and modulus of 22.5 % and 31.7 %, respectively was obtained by the addition of 2 % CNFs. Furthermore, storage modulus was 22.3 % higher than neat epoxy for 2 % loading of CNFs at room temperature, while $T_g$ improved by 18 %. Thermal stability of composite was improved probably due to the catalytic effect of CNFs. Cellulose nanofibers (CNFs) enhanced both first and second decomposition temperatures by up to 19 and 14 °C, respectively over neat system.

**Keywords:** Cellulose nanofibers, Ball milling, Epoxy polymer, Glass transition temperature, Decomposition.

## 1. Introduction

Now a day, development of nanomaterials has drawn wide attention of the researchers all over the world. Numerous research studies have been conducted to develop nanomaterials for various engineering applications such as automotive components, building construction materials, electronic devices, and also for biomedical applications. Unfortunately, most of these nanomaterials fail to satisfy the concept of sustainability. Therefore, researchers are trying to develop bio-based renewable nanomaterials of high mechanical and thermal properties as replacement materials. Cellulose is an important component of lignocellulosic fibers, which consists of a bundle of cellulose nanofibers (CNFs). Several research studies have been conducted to isolate cellulose nanofibers from plant based materials [1-5]. Scientists and engineers are working together to utilize cellulose nanofibers in various engineering applications.

Cellulose nanofibers have shown excellent mechanical properties (high specific strength and modulus), better biodegradability, high aspect ratio,

renewability, large specific surface area, low coefficient of thermal expansion, environmental benefits, low cost and availability [5-7]. These properties of CNFs make them comparable with other engineering materials such as carbon nanotube, carbon nanofibers, graphene nanoplatelets and nanoclay. CNFs have been considered as effective reinforcing materials for fabrication of green composite materials because of higher mechanical properties and their web-like structure.

One of the main disadvantages of using CNFs as reinforcing filler in the polymer matrix is moisture absorption and tendency to be agglomerated. The interaction of hydroxyl groups result in strong hydrogen bond formation between the fibers and also with the moisture. Hydrophilic CNFs show poor dispersion capability in hydrophobic polymer matrix [8]. Therefore, several research studies have been conducted to modify the surface to make them suitable for both hydrophilic and hydrophobic polymer matrix [9-10].

Cellulose nanofibers (CNFs) can be used as filler materials in a wide range of thermosetting polymers such as epoxy and polyester [11-12]. Among the thermosetting polymers, epoxy is a high performance polymer that has applications ranging from rocket casing to dental filling. Incorporation of CNFs into epoxy polymer matrix has shown to improve mechanical properties such as fatigue resistance, high strength and stiffness of the materials [13-14]. Nevertheless, the main drawback of epoxy/CNFs composite is the poor adhesion capability of CNFs that causes poor dispersion into the matrix. Therefore, several techniques such as surface modification as well as solvent exchange methods have been used to increase the adhesion ability of CNFs [8, 15].

In the present study, cellulose nanofibers (CNFs) were extracted from wheat straw by delignification and bleaching treatment followed by ball milling technique for use as reinforcing materials in an epoxy polymer. Surface of CNFs was modified by treating it with silane coupling agent. These CNFs were added to epoxy polymer at different loading to fabricate polymer composites. The fabricated composites were characterized by using SEM, Flexure, DMA, FTIR and TGA.

## 2. Materials and Experiments

### 2.1. Materials

SC-15 Epoxy, a commercially available low viscosity resin (300 cps), purchased from Applied Poleramic, Inc. was used. It is two phase resin containing part-A (mixture of diglycidyl ether of bisphenol A and aliphatic diglycidyl ether epoxy toughener) and part B (hardener, mixture of cycloaliphatic amine and polyoxyl alkyl amine). Wheat straw was purchased from Home Depot, USA. Hydrogen peroxide (30 wt. % in $H_2O$), ethanol (≥ 99.5 %), formic acid (≥ 95 %), sodium hydroxide pellets, silane coupling agent (3-aminopropyltriethoxysilane), methanol (anhydrous, 99.8 %) and acetic acid (ACS reagent, ≥ 99.7) were purchased from Sigma–Aldrich (St. Louis, MO, USA).

### 2.2. Pretreatment of Wheat Straw

Cellulose was extracted from wheat straw according to Nuruddin, *et al.* [16]. In brief, wheat straw and 90 % formic acid were placed on a hot plate maintained at 110 °C for 2 hours. At the end of the reaction time, the fibers were filtered in a Buchner funnel and washed with formic acid followed by hot distilled water. Resulting pulp was further treated with peroxyformic acid solution in hot water bath at 80 °C for 2 hours to remove amorphous content (lignin, hemicellulose and pectin). Finally, delignified fibers were filtered to separate cooking liquor (lignin and hemicellulose mixed with formic acid) from cellulose and washed several times with hot water. Delignified fibers were subjected to bleaching by treating them with 35 % $H_2O_2$ solution and NaOH solution (to maintain pH: 11-12), and kept in a hot water bath at 80 °C for 2 hours. Finally, the pulp was washed several times with distilled water to ensure complete removal of residual lignin.

### 2.3. Isolation of Cellulose Nanofibers (CNFs)

In our laboratory, a new technique has been developed to isolate CNFs by ball milling [17]. Approximately 10 gm of bleached cellulose was soaked in 10 ml of 80 % ethanol solution and the fiber was subjected to milling for 120 minutes in a Mixer/Mill 8000D™ (SPEX Sample Prep, USA) using zirconia ceramic grinding vial and ball with diameter 12.7 mm. After ball milling, the mixture was repeatedly washed with distilled water and centrifuged until the pH of the cellulose reaches between 6 and 7. Finally, the suspension of ball milled cellulose nanofibers (CNFs) was freeze dried.

### 2.4. Surface Modification of Cellulose

1 % silane coupling agent (total weight of fiber) was mixed with 80/20 v/v ethanol/water mixture and then 5 g freeze dried CNFs was added to the mixture. 1 % acetic acid was added dropwise to maintain PH near 3.5, and then the mixture was magnetically stirred at 500 rpm for 90 minutes, maintaining the room temperature. After completion of the reaction, the CNFs suspensions were repeatedly centrifuged and washed with distilled water until the PH became 6. Then samples were freeze dried to use it as filler materials.

### 2.5. Fabrication of Nanocomposites

Precalculated amount of part-A and CNFs were mixed manually in a beaker and then ultrasonicated for 20 minutes at 40 °C, using "Sonics Vibra-cell" (Sonics & Materials Inc., USA) set at 30 seconds pulse on, 20 seconds pulse off, and amplitude of 50 μ. Then the sonicated mixture was magnetically stirred at 500 rpm for 5 hours at 40 °C temperature to ensure complete dispersion of CNFs in the polymer matrix. After that, part B was mixed with part A modified with CNFs in the ratio of 10:3 (part A: part B). The resultant mixture was stirred again using high speed mechanical stirrer for 5 minutes to ensure complete mixing. Then the mixture was kept in a vacuum oven to remove bubbles formed during mixing of part A and part B. After removal of bubbles, the resin was poured into the metal molds for desired shape and kept in an oven at 60 °C for 1 hour followed with 120 °C for 3 hours. For neat samples, calculated amount of part A and part B were mixed in the ratio of 10:3 by using mechanical stirrer following the same procedure as mentioned for CNFs modified samples.

### 2.6. Characterization

#### 2.6.1. Flexure Test

Three point bending flexure test was conducted according to ASTM D790-02, using Zwick-Reoll Z 2.5 machine. The test was conducted under displacement control mode with a crosshead speed of 1.2 mm/min. The sample size was 96 mm × 12.5 mm × 4.5 mm (span length × width × thickness). The span length to thickness ratio of 16:1 was maintained, and at least 5 samples of each type nanocomposites were tested at room temperature.

#### 2.6.2. Scanning Electron Microscopy (SEM)

Scanning electron micrograph of ball milled CNFs was taken using JEOL JSM-6400 scanning electron microscope (SEM) at 20 kV accelerating voltage. Morphological studies of neat epoxy and CNFs reinforced epoxy polymer nanocomposites were conducted using JEOL JSM-6400 scanning electron microscope (SEM) at 15 kV accelerating voltage. Surface of each sample was sputtered with a thin layer of gold particle before SEM conducted.

#### 2.6.3. Transmission Electron Microscopy (TEM)

A drop of dilute cellulose nanofibers (CNFs) suspension was deposited on the 300 mesh Formvar/Carbon coated support film grids. The excess liquid was absorbed by a piece of filter paper and then allowed to dry at room temperature. When the sample has been dried, then it was observedusing ZEISS EM10 Transmission Electron Microscope (Thornwood, NY) operated at 60 kV accelerating voltage.

#### 2.6.4. Fourier Transfer-infrared (FTIR) Spectroscopy

Structural characterization was conducted on CNFs, surface treated CNFs, neat epoxy and CNFs reinforced epoxy polymer composite, using Shimadzu FTIR 8400s equipped with MIRacle$^{TM}$ ATR, and samples were scanned from 550-3500 $cm^{-1}$ with a resolution of 4 $cm^{-1}$.

#### 2.6.5. Dynamic Mechanical Analysis

Dynamic Mechanical Analysis (DMA) of nanocomposites was conducted according to ASTM D4065 using TA Instrument DMA Q-800. The tests were performed in a three-point bending mode at an amplitude of 15 μm and oscillation frequency of 1 Hz. The temperature range was 30 to 150 °C at a heating rate of 5 °C/min. The sample size was 60 mm × 12.5 mm × 4.5 mm, and at least 3 samples of each type of composites were tested. Storage modulus and tan-delta as a function of temperature were obtained. Glass transition temperature was obtained from Tan-delta curve.

#### 2.6.6. Thermogravimetric Analysis (TGA)

Thermal stability of polymer nanocomposites and neat epoxy were studied using thermogravimetric analysis Q-500 from TA Instruments Inc. (DE). Approximately 10-12 mg Samples were taken for the test. TG scans were performed at 10 °C/min from 25 - 600 °C under nitrogen environment with a purge flow rate of 60 mL/min.

## 3. Results and Discussion

### 3.1. Morphological Characterization of CNFs and Nanocomposites

Fig. 1 shows the SEM and TEM images of extracted web like CNFs. The maximum and minimum diameters were calculated from TEM images using MaxIm DL5 software. The maximum and minimum diameter of ball milled CNFs were approximately and 45 nm and 17 nm respectively.

### 3.2. Chemical Structure Analysis

FTIR spectroscopy analysis of CNFs and silane treated CNFs was carried out to confirm the chemical reaction between silane coupling agent and cellulose and were shown in Fig. 2.

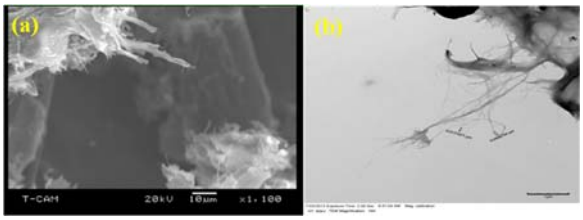


**Fig. 1.** (a) SEM, and (b) TEM images of Cellulose nanofibers (CNFs).

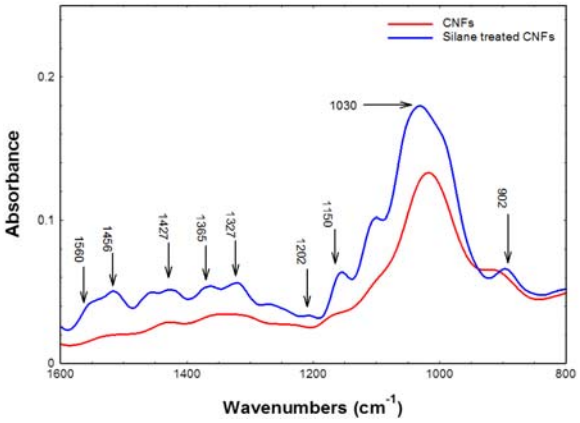


**Fig. 2.** FTIR spectra of CNFs and silane treated CNFs.

Silane treated CNFs show absorption bands at 1560 and 1456 $cm^{-1}$ indicating deformation modes of amino groups ($NH_2$) that are strongly hydrogen bonded with hydroxyl groups of both cellulose and silanol (formed during hydrolysis of silane coupling agent) [13]. The weak peaks at 1427, 1365 and 1327 $cm^{-1}$ represent C-H stretching and C-H or O-H bending [18], which can be seen in untreated and treated cellulose nanofibers. The intense peaks at 1150 and 1202 $cm^{-1}$ represent -Si-O-Si- linkage and -Si-O-Cellulose bonds. -Si-O-Si- bond indicated the existence of polysiloxanes chemically bonded with the cellulose nanofibers and the latter bond proved the condensation reaction between cellulose nanofibers and silane coupling agent as shown in the reaction [19]. The broad peaks at 1030 and 903 $cm^{-1}$ indicative of C-O stretching and C-H deformation vibrations associated with cellulose [20-21], and can be seen in all spectra. The increase in intensity for silane treated CNFs is due to the overlapping of Si-O-Si band and C-O stretching of cellulose [22].

FTIR analysis was also conducted on neat epoxy and silane treated cellulose nanofibers reinforced epoxy polymer composite to understand the chemical structure and chemical reaction (Fig. 3). The broad peak around 3100-3600 $cm^{-1}$ for neat epoxy was due to the O-H stretching vibration of hydroxyl group in epoxy and N-H stretching of primary and secondary amine of hardener. Incorporation of silane treated CNFs into the epoxy system produced a doublet, which was mainly due to the unreacted primary amine groups. The peak at 3042 $cm^{-1}$ is the characteristics peak of C-H stretching of terminal oxirane group of epoxy resin. The peak at 2902 and 2860 $cm^{-1}$ represented the characteristics peaks of C-H stretching of epoxy resin, the intensity of which decreases with addition of CNFs. A peak at 2310 $cm^{-1}$ for both epoxy and epoxy/CNFs was observed, which might be due to double $CO_2$ band [23]. The sharp peak at 1506 $cm^{-1}$ represents the N-H deformation of primary amine of hardener and silane treated CNFs used for epoxy resin. The peaks at 1452 and 1605 $cm^{-1}$ correspond to the aromatic ring stretching of C=C, which is the characteristics of DGEBA epoxy resin. The sharp peaks at 1095 and 1032 $cm^{-1}$ represent the stretching of C-O of saturated aliphatic primary alcohols [24]. These peak intensities decreased with the addition of cellulose nanofibers. The peaks at 1236 and 932 $cm^{-1}$ indicated the stretching of epoxide (-C-O) bonds [25]. Finally, the peak at 823 $cm^{-1}$ was attributed to the stretching of C-O-C of terminal oxirane group of epoxy system.

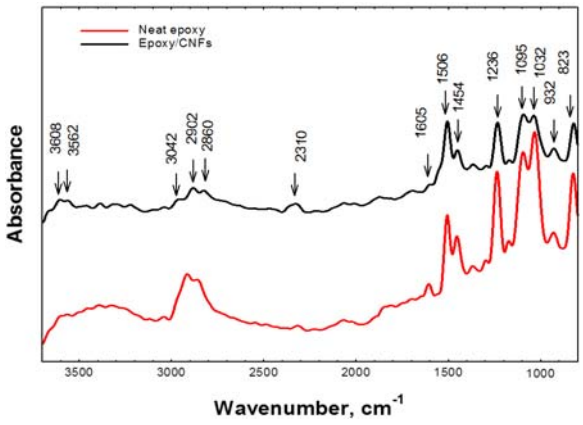


**Fig. 3.** FTIR spectra of neat epoxy and CNFs reinforced epoxy nanocomposites.

### 3.3. Flexure Test

Flexure properties of nanocomposites are characterized by subjecting neat epoxy and CNFs reinforced nanocomposites under three point bending load. The stress-strain curves as shown in the Fig. 4, obtained from flexure test show significant non-linearity, although no remarkable yield point was observed in the curves. Flexure test results obtained from various samples are compared in the Fig. 5.

From Fig. 4, it can be seen that incorporation of cellulose nanofibers into epoxy polymer matrix exhibited significant improvement of flexure strength and modulus. The highest flexure strength and modulus were achieved from 2 % CNFs/epoxy nanocomposite (22.5 % and 31.7 % higher than neat epoxy). In contrast, a reduction in flexure properties at 3 % loading might be due to the strong attractive forces between cellulose nanofibers leading to cluster or agglomeration of CNFs. Due to poor dispersion of CNFs at 3 % loading, CNFs agglomerate in the resin system leading to the reduction of load transfer between CNFs and epoxy polymer.

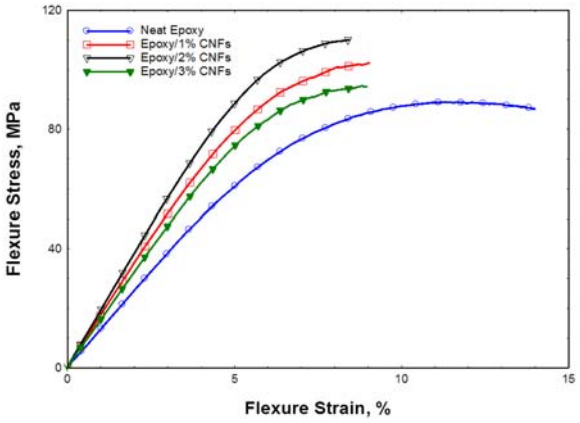


**Fig. 4.** Flexural stress–strain response of neat epoxy and CNFs incorporated epoxy nanocomposites.

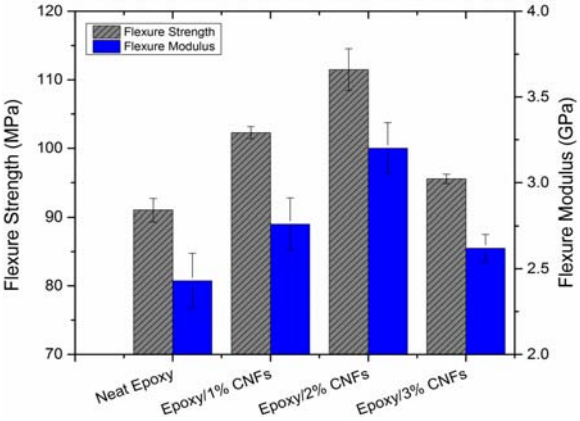


**Fig. 5.** Comparative value of flexure strength and modolus of neat epoxy and CNFs incorporated epoxy nanocomposites.

Uniform dispersion of CNFs ensures more surface area of cellulose nanofibers to be exposed to the matrix and better interaction between CNFs and epoxy polymer. Silane treated CNFs contain amino functional groups that are strong nucleophile. Therefore, these amino functional groups of CNFs get attached to epoxide group of epoxy SC-15 and form strong covalent bond by ring opening reaction. As a result, higher cross-linking between epoxy molecules takes place resulting in an interlocking structure in the matrix reducing the mobility of epoxy polymer chains through the system. Chemically interlocked resin and CNFs structure may facilitate stress transfer between matrix/fiber and fiber/fiber.

Strong covalent bonds between fibers and polymers must be broken before the sample fails while subjecting to loading. Higher crosslinking means formation of higher covalent bonds between fibers and polymer matrix. Hence, flexure strength and modulus of nanocomposites increases after the addition of CNFs. After initiation of crack due to loading, the propagation of the crack gets restricted by the presence of CNFs. Thus, the direction of crack propagation is changed in the presence of CNFs requiring more energy to cause the failure of the composites.

Analysis of failure behavior through scanning electron microscopy of neat epoxy and CNFs modified epoxy polymer composites is presented in Fig. 6. It is apparent from the SEM images that the fracture surface of CNFs modified nanocomposites is rougher than the neat samples. Among the nanocomposites, 2 % CNFs reinforced composites showed roughest fracture surface indicating the highest resistance to crack propagation by the materials. In contrast, the exposed fracture surface of neat epoxy and 3 % CNFs incorporated samples exhibit relatively smoother surface than 2 % CNFs incorporated samples (Fig. 6(a) and Fig. 6(d)). Addition of higher loading causes cluster of agglomerated CNFs. This agglomeration might be due to two factors. One is, 3 % loading CNFs was more than need to crosslink with epoxy polymer resulting in unreacted CNFs in the form of agglomeration. Another important factor is the higher tendency of hydrogen bonding between the hydrogen groups on the surfaces of CNFs. The crack for 3 % CNFs reinforced samples initiated from a zone where the CNFs appear to be agglomerated to form a cluster.

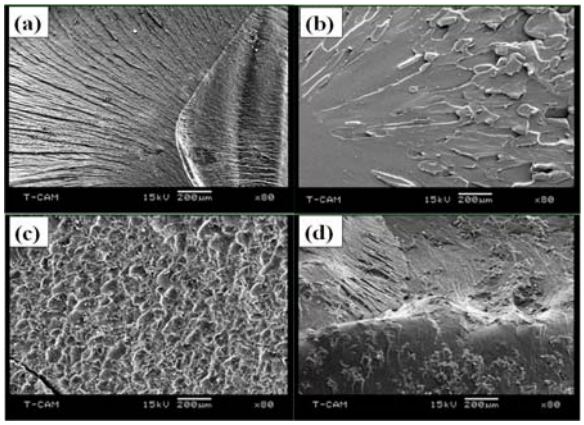


**Fig. 6.** Fracture surfaces of (a) neat epoxy, (b) epoxy/1 % CNFs, (c) epoxy/2 % CNFs and (d) epoxy/3 % CNFs.

### 3.4. Viscoelastic Properties of Epoxy Nanocomposites

The viscoelastic properties of neat epoxy and CNFs reinforced nanocomposites are evaluated as a function of temperature. Fig. 7 and Fig. 8 show the comparison of dynamic mechanical properties such as storage modulus and tan-delta as functions of temperature.

Storage modulus measures the energy stored in the materials after deformation when subjected to cyclic loading. Fig. 7(a) represents the storage modulus of nanocomposites as a function of temperature. From Fig. 8, it can be seen that the addition of CNFs increases the storage modulus as compared with neat epoxy. Maximum storage modulus was achieved for 2 % loading of CNFs (22.3 % higher than neat epoxy) at room temperature. The polymer chains deform with

increasing temperature leading to decrease in stiffness. As mentioned earlier, CNFs form covalent bonds with epoxy polymer by crosslinking that restrict the movement of the polymer chains. In contrast, lower value of storage modulus for 3 % loading of CNFs can be attributed the agglomeration of CNFs.

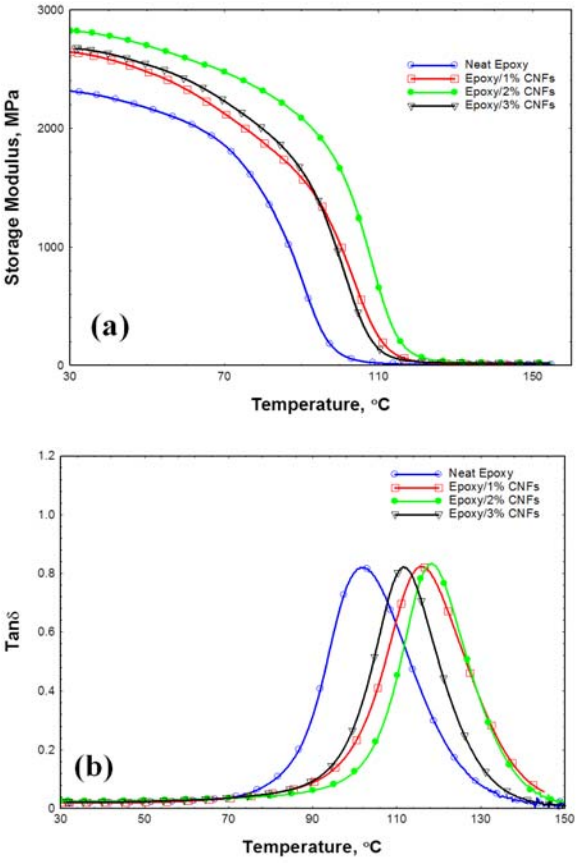


**Fig. 7.** (a) Storage modulus versus temperature curve and (b) Tanδ versus temperature curves of neat epoxy and epoxy/CNFs nanocomposites.

Fig. 7(b) shows the Tan-delta curve of neat epoxy and different percentage of CNFs incorporated epoxy composite samples. Tan-delta value represents the damping properties of the materials and can be expressed as the ratio of loss modulus over storage modulus. The peak of tan-delta curve represents the glass transition temperature ($T_g$). From Fig. 8, it can be observed that the value of $T_g$ increases with the addition of CNFs up to 2 %. About 18 % improvement of $T_g$ was achieved at 2 % loading of CNFs compared with neat epoxy polymer composite. Good dispersion of CNFs was achieved for 2 % loading CNFs into the polymer matrix leading to sufficient crosslinking between matrix and cellulose nanofibers and ensures severe restriction of movement of polymer chain when temperature increases. Thus, the matrix/CNFs crosslinked network initiates to move at a relatively higher temperature than neat epoxy sample leading to higher $T_g$ value. Salam, *et al.* reported that improved interfacial bonding between CNTs and epoxy polymer leads to higher $T_g$ value [26]. At higher loading of CNFs, $T_g$ value was lower possibly because of agglomeration tendency of CNFs.

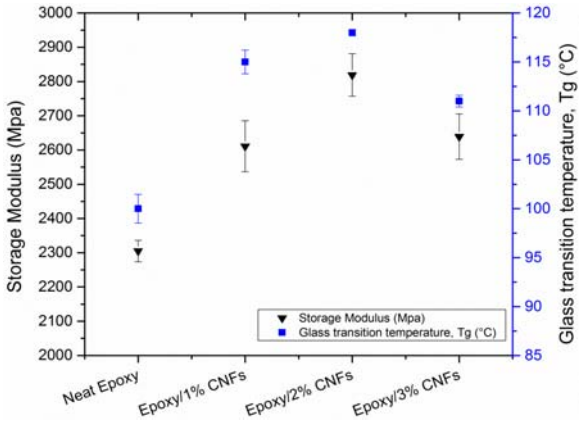


**Fig. 8.** Comparative study of storage modulus and glass transition temperature ($T_g$) of nanocomposites.

## 3.5. Thermal Stability of Nanocomposites

Thermal stability of neat epoxy and cellulose nanofibers incorporated epoxy polymer composites was evaluated by thermo-gravimetric analysis (TGA). Summary of thermal stability of all samples are evaluated in terms of onset of decomposition, (Ti) and maximum decomposition temperature as shown in Table 1. From Table 1 and Fig. 9, it can be seen that the onset temperature varied significantly with the addition of CNFs into epoxy polymer matrix.

**Table 1.** Thermal properties of neat epoxy and CNFs incorporated epoxy nanocomposites.

| Sample | Onset Temperature, Ti (°C) | Maximum Decomposition Temperature (°C) | |
|---|---|---|---|
| | | $T_1$ max | $T_2$ max |
| **Neat** | 311 ± 2.3 | 323 ± 4.2 | 362 ± 6.5 |
| **1 % CNFs/Epoxy** | 319 ± 0.8 | 330 ± 0.5 | 366 ± 3.5 |
| **2 % CNFs/Epoxy** | 327 ± 2.9 | 342 ± 2.6 | 376 ± 4.1 |
| **3 % CNFs/Epoxy** | 323 ± 1.7 | 335 ± 0.9 | 365 ± 6.5 |

Onset temperature of neat epoxy was 311 °C and increased up to 327 °C after incorporation of CNFs.

From DTG curves shown in Fig. 9(b), the decomposition of all samples show two distinct peaks. The first decomposition peak was noticed around 323-342 °C with 13-26 % weight loss, which was mainly due to the decomposition of lower molecular weight materials. The second decomposition peak was around 362-376 °C with 48-60 % weight loss of the samples, which was the result of decomposition of highly

crosslinked materials [27]. Cellulose nanofibers (CNFs) enhance both first and second decomposition temperature with a maximum of 19 and 14 °C respectively over neat system. This improvement of thermal stability can be attributed to the probable catalytic effect of CNFs that enhances the cross-linking reaction between polymers and curing agent [13].

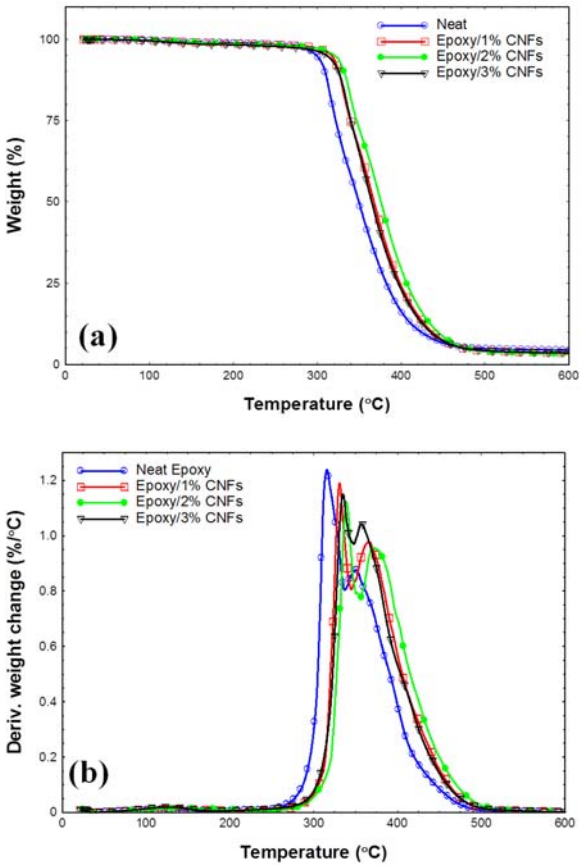


**Fig. 9.** (a) TG, and (b) DTG curves of neat epoxy and epoxy/CNFs nanocomposites.

## 4. Conclusions

In this study, silane treated cellulose nanofibers were incorporated into the DGEBA epoxy resin in order to improve both mechanical and thermal properties of nanocomposites. The chemical reaction and structural analysis was evaluated by FTIR analysis. Incorporation of CNFs into matrix increases flexure strength, flexure modulus, storage modulus, glass transition temperature and decomposition temperatures. Maximum improvement was observed for 2 % loading of CNFs as it facilitates maximum crosslinking with epoxy polymers. The highest flexure strength and modulus were improved by 22.5 % and 31.7 % after addition of 2 % CNFs. Furthermore, storage modulus was 22.3 % higher than neat epoxy for 2 % loading of CNFs at room temperature, while $T_g$ was improved approximately 18 %. Thermal stability of composite was improved probable due to the catalytic effect of CNFs. Cellulose nanofibers (CNFs) enhance both first and second decomposition temperature with a maximum of 19 and 14 °C respectively over neat system.

## Acknowledgements

The authors are grateful to the NSF-CREST (grant No. 1137681) and NSF-EPSCoR (grant No. 1158862) for the financing support to carry out this research.

## References

[1]. F. W. Herrick, R. L. Casebier, J. K. Hamilton, K. R. Sandberg, Microfibrillated cellulose: morphology and accessibility, *J. Appl. Polym. Sci.: Appl. Polym. Symp.; (United States)*, ITT Rayonier Inc., Shelton, WA, 1983.

[2]. N. Hayashi, T. Kondo, M. Ishihara, Enzymatically produced nano-ordered short elements containing cellulose Iβ crystalline domains, *Carbohydrate Polymers*, Vol. 61, No. 2, 2005, pp. 191-197.

[3]. T. Saito, S. Kimura, Y. Nishiyama, A. Isogai, Cellulose nanofibers prepared by TEMPO-mediated oxidation of native cellulose, *Biomacromolecules*, Vol. 8, No. 8, 2007, pp. 2485-2491.

[4]. W. Chen, H. Yu, Y. Liu, P. Chen, M. Zhang, Y. Hai, Individualization of cellulose nanofibers from wood using high-intensity ultrasonication combined with chemical pretreatments, *Carbohydrate Polymers*, Vol. 83, No. 4, 2011, pp. 1804-1811.

[5]. M. A. S. Azizi Samir, F. Alloin, A. Dufresne, Review of recent research into cellulosic whiskers, their properties and their application in nanocomposite field, *Biomacromolecules*, Vol. 6, No. 2, 2005, pp. 612-626.

[6]. W. J. Orts, J. Shey, S. H. Imam, G. M. Glenn, M. E. Guttman, J.-F. Revol, Application of cellulose microfibrils in polymer nanocomposites, *Journal of Polymers and the Environment*, Vol. 13, No. 4, 2005, pp. 301-306.

[7]. T. Nishino, I. Matsuda, K. Hirao, All-cellulose composite, *Macromolecules*, Vol. 37, No. 20, 2004, pp. 7683-7687.

[8]. A. Brandt, J. Gräsvik, J. P. Hallett, T. Welton, Deconstruction of lignocellulosic biomass with ionic liquids, *Green Chemistry*, Vol. 15, No. 3, 2013, pp. 550-583.

[9]. M. Abdelmouleh, S. Boufi, M. N. Belgacem, A. Dufresne, A. Gandini, Modification of cellulose fibers with functionalized silanes: effect of the fiber treatment on the mechanical performances of cellulose–thermoset composites, *Journal of Applied Polymer Science*, Vol. 98, No. 3, 2005, pp. 974-984.

[10]. X. Li, L. G. Tabil, S. Panigrahi, Chemical treatments of natural fiber for use in natural fiber-reinforced composites: a review, *Journal of Polymers and the Environment*, Vol. 15, No. 1, 2007, pp. 25-33.

[11]. J. W. Gilman, D. L. VanderHart, T. Kashiwagi, Thermal decomposition chemistry of poly (vinyl alcohol), in *Proceedings of the American Chemical Society Symposium Series* 599 *on Fire and Polymers II: Materials and Test for Hazard Prevention*1994, pp. 161-185.

[12]. S. Liang, Q. Huang, L. Liu, K. L. Yam, Microstructure and molecular interaction in glycerol plasticized

chitosan/poly (vinyl alcohol) blending films, *Macromolecular Chemistry and Physics*, Vol. 210, No. 10, 2009, pp. 832-839.
[13]. P.-Y. Kuo, N. Yan, M. Sain, Influence of cellulose nanofibers on the curing behavior of epoxy/amine systems, *European Polymer Journal*, Vol. 49, No. 12, 2013, pp. 3778-3787.
[14]. M. Nuruddin, R. Gupta, A. Tcherbi-Narteh, M. Hosur, S. Jeelani, Synergistic Effect of Graphene Nanoplatelets and Nanoclay on Epoxy Polymer Nanocomposites, *Advanced Materials Research, Trans Tech Publications*, 2015, pp. 155-159.
[15]. A. Valadez-Gonzalez, J. Cervantes-Uc, R. Olayo, P. Herrera-Franco, Effect of fiber surface treatment on the fiber–matrix bond strength of natural fiber reinforced composites, *Composites Part B: Engineering*, Vol. 30, No. 3, 1999, pp. 309-320.
[16]. M. Nuruddin, A. Chowdhury, S. Haque, M. Rahman, S. Farhad, M. S. Jahan, A. Quaiyyum, Extraction and characterization of cellulose microfibrils from agricultural wastes in an integrated biorefinery initiative, *Cellulose Chem. Technol.*, Vol. 45, No. 5-6, 2011, pp. 347-354.
[17]. M. Nuruddin, M. Hosur, M. Uddin, D. Baah, S. Jeelani, A novel approach for extracting cellulose nanofibers from lignocellulosic biomass by ball milling combined with chemical treatment, *Journal of Applied Polymer Science*, Vol. 133, No. 9, 2016, pp. 1-10.
[18]. M. Jiang, M. Zhao, Z. Zhou, T. Huang, X. Chen, Y. Wang, Isolation of cellulose with ionic liquid from steam exploded rice straw, *Industrial Crops and Products*, Vol. 33, No. 3, 2011, pp. 734-738.
[19]. A. N. Frone, D. M. Panaitescu, D. Donescu, C. I. Spataru, C. Radovici, R. Trusca, R. Somoghi, Preparation and characterization of PVA composites with cellulose nanofibers obtained by ultrasonication, *BioResources*, Vol. 6, No. 1, 2011, pp. 487-512.
[20]. A. Alemdar, M. Sain, Isolation and characterization of nanofibers from agricultural residues–Wheat straw and soy hulls, *Bioresource Technology*, Vol. 99, No. 6, 2008, pp. 1664-1671.
[21]. R. Li, J. Fei, Y. Cai, Y. Li, J. Feng, J. Yao, Cellulose whiskers extracted from mulberry: A novel biomass production, *Carbohydrate Polymers*, Vol. 76, No. 1, 2009, pp. 94-99.
[22]. W. Zhang, X. Yang, C. Li, M. Liang, C. Lu, Y. Deng, Mechanochemical activation of cellulose and its thermoplastic polyvinyl alcohol ecocomposites with enhanced physicochemical properties, *Carbohydrate Polymers*, Vol. 83, No. 1, 2011, pp. 257-263.
[23]. Y. Yamashita, C. Sasaki, Y. Nakamura, Development of efficient system for ethanol production from paper sludge pretreated by ball milling and phosphoric acid, *Carbohydrate Polymers*, Vol. 79, No. 2, 2010, pp. 250-254.
[24]. Y. Nishiyama, J. Sugiyama, H. Chanzy, P. Langan, Crystal structure and hydrogen bonding system in cellulose Iα from synchrotron X-ray and neutron fiber diffraction, *Journal of the American Chemical Society*, Vol. 125, No. 47, 2003, pp. 14300-14306.
[25]. M. S. Jahan, A. Saeed, Z. He, Y. Ni, Jute as raw material for the preparation of microcrystalline cellulose, *Cellulose*, Vol. 18, No. 2, 2011, pp. 451-459.
[26]. M. Salam, M. Hosur, S. Zainuddin, S. Jeelani, Improvement in Mechanical and Thermo-Mechanical Properties of Epoxy Composite Using Two Different Functionalized Multi-Walled Carbon Nanotubes, *Open Journal of Composite Materials*, Vol. 3, No. 2A, 2013, pp. 1-9.
[27]. S. Zainuddin, M. Hosur, Y. Zhou, A. T. Narteh, A. Kumar, S. Jeelani, Experimental and numerical investigations on flexural and thermal properties of nanoclay–epoxy nanocomposites, *Materials Science and Engineering: A*, Vol. 527, 2010, pp. 7920-7926.